

UNCLASSIFIED

Defense Technical Information Center
Compilation Part Notice

ADP012302

TITLE: Electrochemical Deposition of FeCo Alloys and FeCo/TiO₂
Nanocomposites

DISTRIBUTION: Approved for public release, distribution unlimited

This paper is part of the following report:

TITLE: Applications of Ferromagnetic and Optical Materials, Storage and
Magnetoelectronics: Symposia Held in San Francisco, California, U.S.A. on
April 16-20, 2001

To order the complete compilation report, use: ADA402512

The component part is provided here to allow users access to individually authored sections
of proceedings, annals, symposia, etc. However, the component should be considered within
the context of the overall compilation report and not as a stand-alone technical report.

The following component part numbers comprise the compilation report:

ADP012260 thru ADP012329

UNCLASSIFIED

Electrochemical Deposition of FeCo Alloys and FeCo/TiO₂ Nanocomposites

I. Shao^a, P. M. Vereecken^a, R. C. Cammarata^a, P. C. Searson^a, and C. L. Chien^b

^aDepartment of Materials Science and Engineering
The Johns Hopkins University, Baltimore, MD 21218

^bDepartment of Physics and Astronomy
The Johns Hopkins University, Baltimore, MD 21218

ABSTRACT

Electrochemical deposition of FeCo alloys with 1:1 atomic ratio has proved difficult due to cracking from high stress. By using a sulfamate electrolyte and optimizing other deposition parameters, we successfully electrodeposited high quality FeCo films of 20-25 μm in thickness and 7 mm in diameter. Using a suspension of hard oxide nanoparticles (25 nm TiO₂) in the electrolyte, we produced oxide-dispersion-strengthened FeCo/TiO₂ nanocomposite films with large grains. Enhanced strength was observed from these nanocomposites relative to pure FeCo alloys as determined from Knoop hardness measurements. In order to further improve the ductility of the alloys, vanadium has been codeposited with FeCo. Some preliminary results of FeCoV alloy deposition are reported.

INTRODUCTION

Iron-cobalt alloys near the equiatomic composition have superior soft magnetic properties with a very high saturation magnetization (24 kG), high permeability at high magnetic flux density, and low D.C. coercivity. In the field of micro-devices, such as hard disk drives, micro-actuators and micro-inductors, thin film deposition processes have to be developed to generate desirable magnetic materials. Electrochemical deposition is an important processing technology for microfabrication due to its low cost, high yield, low energy requirements, and capability for generating high-aspect-ratio features. However, electrochemical deposition of FeCo alloys has been problematic over the years.

Bulk FeCo alloys are primarily used in the manufacture of rotor and stator laminations in motors and generators for aircraft power generation applications. The inferior mechanical properties of these alloys, including low yield strength, low creep resistance, and poor ductility, inhibit many applications. Oxide dispersion strengthening can improve both yield strength and creep resistance. We have utilized electrochemical codeposition from an electrolyte containing a suspension of TiO₂ particles (25 nm in diameter) to produce oxide dispersion strengthened FeCo/TiO₂ nanocomposites. Large grain sizes of the order of 10 μm were observed for all these FeCo/TiO₂ films. Composition, hardness and magnetic properties were tested for these films.

EXPERIMENTAL

FeCo alloy films were deposited from an aqueous sulfamate solution of 0.75 M cobalt sulfamate (IMC Americhem) + 0.5 M iron(II) sulfamate (Strem Chemicals) + 0.4 M boric acid + 0.25 M sodium chloride + 0.025 M sodium borate + 0.025 M vitamin C + 1 g/l saccharine + 0.5 vol.% aerosol DPOS 45 surfactant (Cytec Industries) + 0.4 mM ammonium metavanadate. A small amount of vanadium was added to enhance the ductility of the alloy. Although no vanadium was detected in the deposited films (the detection limit of wavelength dispersive spectroscopy (WDS) was 0.1 wt.%), it was found that this solution produced more ductile films

than films produced from the vanadium-free electrolyte. The pH of the solution was about 4. After preparation the solution was kept under a nitrogen atmosphere at all times. The bath temperature was kept at 50 °C during deposition. Hipercor FeCo50 (Fe₄₉Co₄₉V₂ by weight) alloy from Carpenter Technology Corporation was used as the counter electrode. The counter electrode was separated from the working electrode with glass frit.

25 nm in diameter TiO₂ particles (Degussa P25) were added to the solution to make 0.1 vol.% TiO₂ suspensions for deposition of FeCo/TiO₂ nanocomposite films. The solution was stirred for at least one hour to make a stable suspension. The composition of FeCo and FeCo/TiO₂ films was determined by wavelength-dispersive spectroscopy (WDS), using a JXA-8600 SuperProbe. An anatase standard was used to calibrate the TiO₂ spectrum. Pure Fe, Co metal standards were used for calibration of Fe and Co spectrums. Knoop hardness was tested on all the films with a Leco M-400 microhardness tester using a load of 50 g. Magnetic hysteresis loops were measured using a vibrating sample magnetometer (VSM). Both atomic force microscopy (AFM) and scanning electron microscopy (SEM) images were used to investigate the microstructure and morphology of the films..

In order to codeposit more vanadium with FeCo, we replaced ammonium metavanadate (0.4 mM) in the solution with the more soluble vanadyl sulfate (50 mM VOSO₄). The FeCoV deposition solution is made of 0.5M iron sulfamate + 0.5M cobalt sulfamate + 0.4 M boric acid + 0.25 M sodium chloride + 0.025 M sodium borate + 0.025 M vitamin C + 1 g/l saccharine + 0.5 vol.% aerosol DPOS 45 surfactant (Cytec Industries) + 50 mM vanadyl sulfate. The pH was adjusted to 4 with sodium hydroxide. About 1 - 2 atomic percent of vanadium was detectable from energy dispersion x-ray spectroscopy (EDS) measurements. Hysteresis loops were measured for these FeCoV alloy films.

RESULTS AND DISCUSSIONS

FeCo alloy deposition

A series of FeCo alloy films were deposited at constant current densities of -5, -10, -20, -40, -100, -200, and -400 mA/cm² and at a rotation rate of 1000 rpm. The composition of FeCo as determined from WDS is plotted as a function of current density in figure 1. It can be seen that a Fe composition close to 50 at.% was achieved between -20 and -40 mA/cm². At higher current densities, a Fe composition of about 47 wt.%, independent of current density, was observed. At lower current densities, the film composition was strongly dependent on current density. The Fe²⁺ to Co²⁺ ratio in the solution was 2:3, whereas the ratio of Fe to Co in the deposits was about 1:1 for films formed at current densities higher than -10 mA/cm². Contrary to what would be anticipated from the equilibrium potentials for the single Fe²⁺/Fe and Co²⁺/Co redox couples (Fe is less noble than Co), Fe deposition was much faster than Co at those current densities. Such anomalous codeposition of Fe and Co is a common phenomenon for electrodeposition of iron group alloys ⁽¹⁾.

The microstructure of the FeCo films was studied using AFM. Figure 2 shows an AFM image of an as-deposited FeCo film (-20 mA/cm², 1000 rpm). The deposited films were very smooth and the grain size was about 150-250 nm in diameter. Similar submicron grains were observed for all the other FeCo films deposited between -5 and -400 mA/cm².

Magnetic hysteresis loops were measured for these samples. The saturation magnetization was normalized to the volume of FeCo material in the film, which was calculated from the total charge passed during deposition, the film composition and the deposition efficiency for each

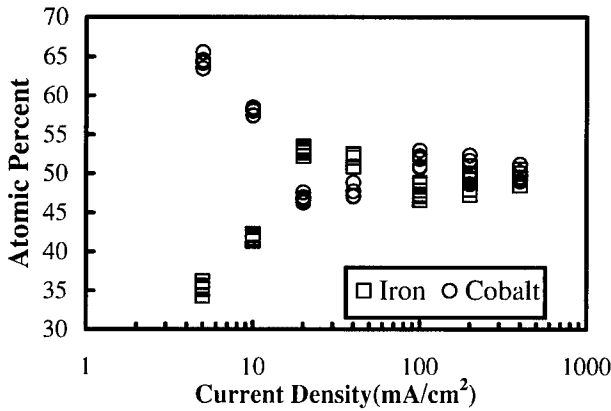


Figure 1. FeCo alloys composition as a function of deposition current density. Two samples were made at each current density. The $\text{Fe}^{2+}:\text{Co}^{2+}$ ratio in the electrolyte was 2:3.

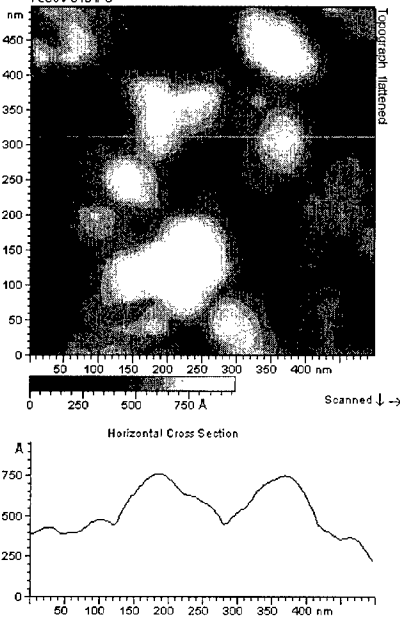


Figure 2. AFM image of an as-deposited FeCo film made at -20 mA/cm^2 and 1000rpm.

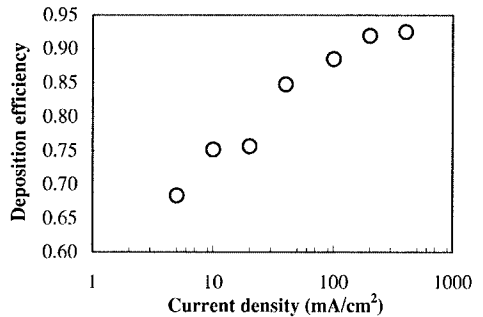


Figure 3. Deposition efficiencies of FeCo alloys versus deposition current density.

current density. Deposition efficiency is plotted as a function of current density in figure 3. It can be seen that deposition efficiency increases with increasing current density. Table 1 shows the saturation magnetization and coercivity of FeCo films together with the deposition efficiency and the film composition.

Knoop hardness tests were carried out with a load of 50 g on films polished with $0.05 \mu\text{m}$ Al_2O_3 paste. Table 1 also shows the hardness results for all FeCo films. It can be seen that hardness was not a sensitive function of film composition in the range of 33 - 51 wt.% Fe.

Table 1. Magnetic properties, deposition efficiency, and hardness of FeCo films deposited at different current densities.

Current density(mA/cm ²)	-5	-10	-20	-40	-100	-200	-400
Fe wt.%	33	38	51	50	46	47	47
Current efficiency	68%	75%	76%	85%	89%	92%	93%
4πM _s (kG)	20.6	21.0	21.8	21.1	21.3	21.6	21.6
H _c (Oe)	33	29	12	16	6	6	8
Hardness (Gpa)	3.1	3.1	3.8	4.1	3.1	3.2	3.2

FeCo/TiO₂ deposition

A Fe / Co ratio of 1:1 was achieved for films deposited at current densities between -20 and -40 mA/cm². A series of FeCo/TiO₂ samples were deposited at a current density of -20 mA/cm² with different rotation rates. A concentration of 1 to 2 vol.% TiO₂ (25 nm in diameter) in the films was observed for films deposited from 0.1 vol.% TiO₂ solution. The Fe / Co ratio of these films was lower than pure FeCo alloys deposited with the same conditions and close to the electrolyte ion ratio. Apparently the presence of TiO₂ nanoparticles in the electrolyte inhibits the anomalous codeposition of Fe and Co as observed in the solution without TiO₂ particles.

Grain sizes of order of 10 μm were observed for all FeCo/TiO₂ nanocomposite films. Figure 4 shows a typical SEM image for an as-deposited FeCo/TiO₂ film deposited at 2000 rpm and -20 mA/cm² from 0.1 vol.% TiO₂ solution. The average grain size was estimated to be 8 μm.

The hardness of the nanocomposite films is plotted as a function of rotation rate in figure 5. It can be seen that hardness increases as rotation rate. This is due to the increasing amount of embedded particles in the films when the rotation rate was increased. Similar behavior has been reported for the Ni/Al₂O₃ system⁽²⁾.

The hardness of the electrodeposited FeCo/TiO₂ nanocomposites was compared to cast Hipercor FeCo alloys. The hardness of the electrodeposited FeCo/TiO₂ (1 to 2 vol.%) nanocomposites were on average 50% higher than the similar grain size Hipercor FeCo alloys from the Hall-Petch relation reported by Shang etc.⁽³⁾.

Magnetic hysteresis loops were measured for all FeCo/TiO₂ films. The saturation magnetization was normalized to the volume of FeCo in the film. Figure 6 shows the magnetic hysteresis loops for a FeCo/TiO₂ nanocomposite film and a FeCo alloy film with a similar Fe:Co ratio. The Fe₄₀Co₆₀/TiO₂ film was made at -20 mA/cm² and 1000 rpm and the Fe₄₀Co₆₀/TiO₂ was made at -10 mA/cm² and 1000 rpm. From the figure, it is seen that the addition of TiO₂ slightly

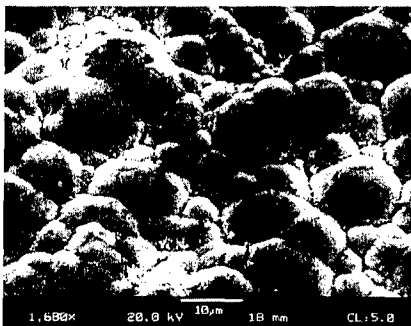


Figure 4. Scanning electron micrograph of an etched FeCo/TiO₂ nanocomposite film deposited from a 0.1 vol.% TiO₂ solution at 2000 rpm and -20 mA/cm².

degraded the saturation magnetization, but improved the squareness of hysteresis loop. This can be attributed to a combined effect of grain size and nanoparticles incorporation.

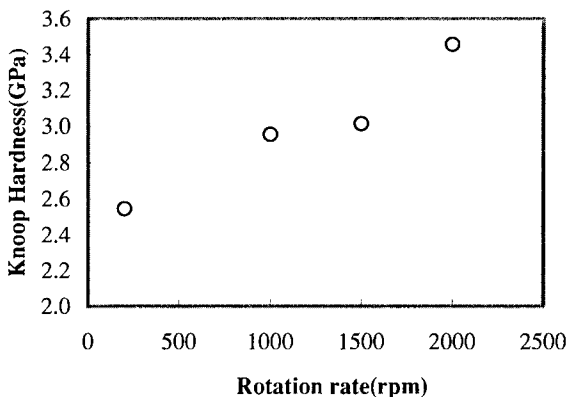


Figure 5. Hardness of the FeCo/TiO₂ nanocomposites deposited from 0.1 vol.% TiO₂ solutions.

FeCoV alloy deposition

Vanadium proved to be a very effective element that improved the ductility of FeCo alloys⁽⁴⁾. We attempted codepositing more V into the films by using a more soluble V salt VOSO₄. Figure 7 compares three i-U curves obtained from blank (a), V-only (b) and FeCoV (c) deposition solutions. Ammonium sulfamate replaced Fe sulfamate and Co sulfamate to make the blank solution, and VOSO₄ was added to the blank solution to make the V-only solution. All solutions were freshly made and kept under nitrogen atmosphere at all times. The i-U curve from the V-only solution shows two plateaus in the deposition stage compared to the blank solution. This may be due to the reduction of high valence V ions to lower valence V ions in the solution. By introducing Fe and Co ions into the electrolyte, we could still distinguish a similar plateau in the i-U curve. Very nice deposition and stripping peaks can be seen from figure 7 (c) from the FeCoV electrolyte.

A series of FeCoV samples with 7 mm in diameter were made at -20 mA/cm² and 1000 rpm. The samples were weighed before and after deposition to calculate the weight of the deposit. The films were smooth and highly reflective. The film composition was Fe₅₃Co₄₆V₁ measured with EDS. Deposition efficiency was calculated from the film weight and film composition. A value of 80% deposition efficiency was consistently obtained for all the samples. The film thickness was approximately 22 μm as calculated from the passed charged, taking into account the current efficiency.

Magnetic properties of FeCoV films were measured with VSM. A saturation magnetization value of 22 kGauss and a coercivity of 7 Oe were observed.

SUMMARY

We successfully produced high quality Fe₅₀Co₅₀ films electrochemically. Oxide dispersion strengthened FeCo/TiO₂ nanocomposite films were made by using FeCo electrolyte with a TiO₂ suspension. Hardness enhancement was observed due to particle incorporation. The TiO₂ particles played an important effect on the kinetics of the deposition as well as on the microstructure of the films. FeCoV alloy deposition was also perfected. Further investigation of

FeCoV codeposition and scaling-up the deposition cell to produce large samples is currently being conducted.

ACKNOWLEDGMENTS

This work was supported by DARPA and NSF/MRSEC (DMR 96-35526).

REFERENCES

1. Abner Brenner, *Electrodeposition of Alloys*, Academic Press, 1963.
2. P.M. Vercecken, I. Shao, P.C. Searson, *J. Electrochem. Soc.*, **147** (7), 2572-2575, (2000).
3. C.H. Shang, R.C. Cammarata, T.P. Weihs, C.L. Chien, *J. Mater. Res.* **15**(4), 835 (2000).
4. R.M. Bozorth, *Ferromagnetism*, Institute of Electrical & Electronics, 1983.

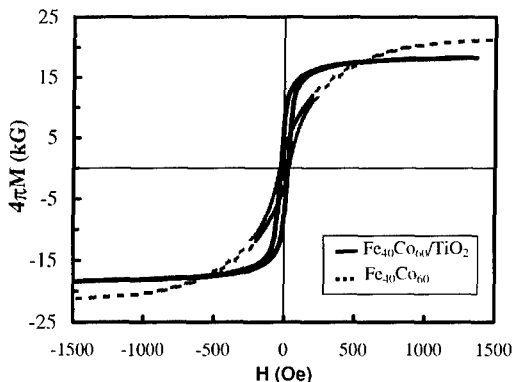


Figure 6. Magnetic hysteresis loops for $\text{Fe}_{40}\text{Co}_{60}/\text{TiO}_2$ (-20 mA/cm^2 and 1000 rpm), and $\text{Fe}_{40}\text{Co}_{60}$ (-10 mA/cm^2 and 1000 rpm) films.

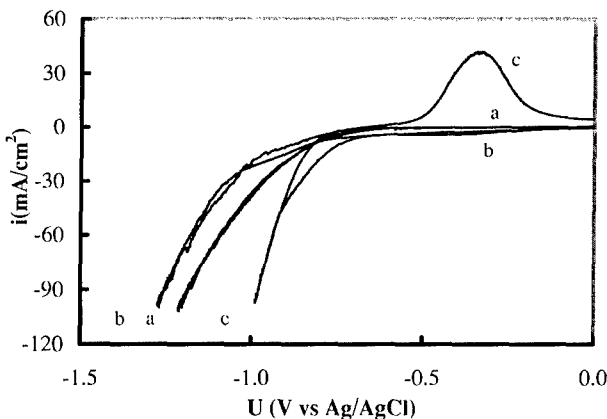


Figure 7. *i*-*U* curves from (a) blank solution, (b) V-only solution and (c) FeCoV solution.